Sleep structure and quantity are determined by behavioral transition probability in *Drosophila melanogaster*

Timothy D. Wiggin[1], Patricia R. Goodwin1, Nathan C. Donelson[2,#], Chang Liu[1], Kien Trinh[2], Subrahata Sanyal[2,##], and Leslie C. Griffith[1]*

[1] Department of Biology, National Center for Behavioral Genomics and Volen Center for Complex Systems, Brandeis University, Waltham, MA, 02454-9110 USA
[2] Biogen, Cambridge, MA
[#] Current address: Department of Cell Biology, Harvard Medical School, Boston, MA
[##] Current address: Calico Labs, South San Francisco, CA

***Correspondence:**
Leslie C. Griffith
Brandeis University
Department of Biology MS008
415 South Street,
Waltham, MA, 02454-9110, USA
Tel: 781 736 3125
griffith@brandeis.edu

Acknowledgements

We would like to thank Dr. Jané Kondev and the students in the Brandeis Quantitative Biology Research Community (QBReC) who assisted in collecting preliminary data.

Grants

This work was funded by R01 MH067284 (to LCG) and F32 NS098624 (to TDW).

ABSTRACT

In humans and flies, sleep is a highly organized behavior, occurring in discrete episodes that are consolidated at night but have a more fragmented structure during the day. Longer episodes correlate with transitions to deeper sleep states for both species, and sleep fragmentation has been shown to have deleterious outcomes for a large number of physiological processes. In mammals and birds, EEG provides an excellent measure of sleep structure and state. In invertebrates, assessment of sleep structure has relied on measures of episode duration, which can fail to capture important aspects of sleep architecture. Here we model *Drosophila* sleep as a probabilistic behavior and develop analytical tools to measure transition probabilities and the organization of sleep episodes within a defined analysis window. We show that these tools provide insight into the underlying mechanisms of normal sleep and into how they are altered in pathological conditions. The probability of transition to the wake state, P(Wake), is a major driver of normal sleep quantity and is responsive to dopaminergic tone, suggesting it is a measure of arousal. The probability of transition to the sleep state, P(Doze), is regulated by sleep deprivation and contributes significantly to regulating sleep fragmentation, suggesting it is a measure of sleep drive. Our method for assessing sleep fragmentation adds important information about the organization of sleep bouts that is missing in measures of episode duration alone. Importantly, the ability to measure behavioral drives provides a way to compare the effects of neural circuits and perturbations that play a role in more than one sleep-relevant process.

INTRODUCTION

Sleep is a broadly conserved, restorative, and essential behavior. In many animals, sleep progresses through a sequence of stages with successively higher arousal thresholds (for review see Eban-Rothschild and Bloch, 2012). The length of time spent continuously asleep determines the likelihood of reaching deeper sleep states, which are associated with restorative function (Scammell et al., 2017). Conditions which disrupt long episodes of sleep in mammals are associated with cognitive disruption and poor health outcomes (Baud et al., 2013; Lim et al., 2012; Martin et al., 2016; Qian et al., 2016). There is also evidence that the fruit fly *Drosophila melanogaster* has sleep stages, with deep sleep stages only occuring during long sleep bouts (Nitz et al., 2002; van Alphen et al., 2013; Yap et al., 2017), and sleep has been shown to be important for memory formation (Berry et al., 2015; Donlea et al., 2011). The neural mechanisms that regulate sleep episode duration and the transitions between sleep and wake are therefore of significant clinical and basic science interest.

Transitions between sleep and wake can appear sharp and switch-like. In the early 20th century, von Economo argued that the transition between sleep and wake was localized to a single “nervous center” (von Economo, 1930). In contemporary literature, localization of function is still expressed using the idea of "sleep-promoting" or “wake-promoting” cells or neurons. However, far from arising from a single center, there are many interconnected cell groups that participate in sleep transitions in the mammalian brain (Scammell et al., 2017). Even in *Drosophila*, which have much smaller brains, the localization of sleep initiation is complex, with dozens of cellular loci that can, in specific contexts, drive sleep/wake transitions (Tomita et al., 2017). In order to

understand the regulation of sleep, it will be essential to integrate the effects of, and relationships among, the many neurons that have been shown to be able to affect sleep.

One obstacle to obtaining a more holistic view of the distributed sleep circuit is that there is not a metric for comparison of the function of different brain areas or genotypes which captures the structure of sleep or the probabilistic nature of sleep transitions. In this paper we develop new analysis tools that will be useful for assessing both sleep structure and the probabilistic nature of behavioral transitions. We provide a new way to measure sleep fragmentation (the Hamming Index) that captures information about the organization of episodes as well as their duration. We also develop a method for obtaining a global assessment of the state of the sleep system expressed as probabilities of behavioral transitions. This is useful due to the complex nature of sleep circuits/genes and provides a way to compare the “state” of the system between genotypes or treatments. Lastly, we provide evidence that state transition probabilities can be tied to biological processes. We find that P(Wake) is strongly influenced by dopamine, the major neurochemical involved in arousal in *Drosophila* (Andretic et al., 2005; Kume et al., 2005), and that age-dependent changes in sleep (Koh et al., 2006; Vienne et al., 2016) reflect changes in the underlying sleep/wake transition probabilities.

EXPERIMENTAL PROCEDURES

Animals

Flies were raised on cornmeal-dextrose-yeast food in a 25°C incubator. The incubator maintained a 12 hour:12 hour light:dark cycle. Flies were collected 0-2 days post-eclosion and housed in mixed-sex, low-density vials until the beginning of the experiment (typically 12 male and 12 female flies). Female flies used in behavioral experiments were co-housed with males, and were therefore presumably mated. For experiments in which the age of the flies is not specified, flies were 6 – 10 days old at the beginning of data collection. Transgenic flies were as follows: per^{01}(CS) – gift of Michael Rosbash, w^{1118} and w^{1118}; dat^{fmn} – gift of Amita Sehgal, PBac{WH}inc^{f00285}, w^{1118} (inc^{2}; Bloomington Stock Center # 18307).

Sleep Measurements

Flies were briefly anesthetized with CO_2, loaded into glass tubes containing 5% agarose/2% sucrose food, and tubes were mounted in *Drosophila* Activity Monitor (DAM) boards (Trikinetics, Waltham, MA). Experiments were carried out at 25°C with a 12 hour:12 hour light:dark cycle, unless otherwise specified. Flies were given a day to acclimate to the DAM system before data collection began. Sleep deprivation was performed by securing the DAM systems to a motorized vortexer and shaking the flies with an inter-pulse period of 10 seconds and a pulse duration of 2 seconds. Unshaken control flies were housed in the same incubator, but not attached to the vortexer.

Generation of In Silico data

Simulation data was generated by custom programs written in Matlab (MathWorks, Natick, MA). The Markov chain simulation accepted as input the number of simulations, the duration (in time steps) of each simulation, and the values of P(Wake) and P(Doze) for the *in silico* flies. The simulation was initialized in a random state with equal probability of wake and sleep at *time* = 1. At each subsequent time step *i*, the simulator: 1) Generated a random number between 0 – 1, 2) Checked activity at *time*(*i* – 1), 3) Compared the random number with the behavioral transition probability. If the fly was active at *time*(*i* – 1), it was compared with P(Doze). If the fly was inactive, it is compared with P(Wake). 4) If the random number was less than or equal to the appropriate transition probability, the fly switched states. 5) The simulation proceeded to the next time step. The first 100 time steps were discarded to minimize the contribution of the initialization state to the simulation output. The Power-Law simulation proceeded along similar lines, however rather than a single P(Wake) and P(Doze), the power-law function was solved for the behavioral state duration at time = *i*, and the result was compared with the random number 0 – 1. Activity was coded as 1, inactivity was coded as 0.

Sleep Data Analysis

Both DAM system and *in silico* data were analyzed with a common set of modular programs written in Matlab. Raw beam crossing data from the DAM was trimmed to the appropriate experimental time period and binned to 1 minute intervals using DAMFileScan (TriKinetics). The experimental design and fly genotype metadata

were transcribed into a text file. The Matlab program imported the DAM data and metadata. Flies with 13 or more hours of continuous inactivity at the end of an experiment were excluded as potentially dead. Continuous periods of inactivity lasting 5 minutes or longer were classified as sleep (Shaw et al., 2000). Standard sleep measures were calculated as follows: Activity while awake was the total beam breaks divided by the number minutes with activity. Total Sleep was the count of bins classified as sleep. Mean episode duration was the total sleep divided by the number of episodes.

The Hamming index was calculated as follows: the Hamming distance was calculated between the experimental data and every possible fully consolidated equivalent. A fully consolidated equivalent is a sleep record with the same total sleep as the experimental data, but only one sleep episode. The fully consolidated templates were generated iteratively by creating an empty variable of equal length to the experimental window, placing an episode with duration equal to total sleep at the first bin of that variable, and moving the episode through the duration of the variable one bin at a time. The minimum value of Hamming distance between the experimental data and a fully consolidated equivalent is the Hamming Index for that fly. If there was either no sleep or if the fly exclusively slept during the analysis window the Hamming Index is undefined.

Probability of wake, or P(Wake), was calculated as follows: 1) Count every bin of inactivity except the last one. This is the denominator, the total number of state transitions from inactivity. 2) For every bin of inactivity, count the number of times the fly is active in the subsequent bin. This is the numerator, the total number of state transitions from inactive to active. 3) Divide the total state transitions from inactive to

active by the total state transitions from inactive. If there were no bins where the fly does not move (*i.e.*, denominator is zero), the transition probability is undefined. Probability of doze, or P(Doze), was calculated identically, but with activity and inactivity reversed.

Curve fitting was performed using the Matlab curve fitting toolbox using the least absolute residual method. Fit parameters are reported ± the 95% confidence interval. Statistical analysis was performed using the Matlab statistics toolbox, data was tested for main effects using ANOVA, and post-hoc t-tests were corrected using Tukey's Honestly Significant Difference Procedure (hsd).

RESULTS

Conditional Probability and an Information Theory Measure of Sleep

One approach to quantifying the structure of fly sleep is to consider an animal's behavior as switching between two states: active and inactive. Between each observation, the fly may choose to either remain in its current state or switch. The activity pattern of the fly reveals the overall probability of choosing each state, and the conditional probability of switching *e.g*. from active to inactive. We propose to call these conditional probabilities P(Wake), the probability that the fly will switch from the inactive state to the active state, and P(Doze), the probability that the fly will switch from the active state to the inactive state (see *Experimental Procedures* and Fig. 1 for detailed explanation).

We also propose a new method for measuring sleep fragmentation that we call the Hamming distance sleep fragmentation index, or Hamming Index. The most

commonly used method for analyzing sleep fragmentation is based on sleep episode duration or episode count (Andretic and Shaw, 2005; Linford et al., 2012). Episode duration and number of episodes are important features of sleep structure, but information about when the episodes occur is also important. The Hamming Index is the minimum Hamming distance (number of mismatches divided by sequence length, Hamming, 1950) between the behavioral output of the fly and any fully consolidated equivalent – a sleep pattern with the same total duration of sleep that is organized into a single episode. The Hamming index therefore captures data about both the degree to which sleep occurs in long episodes and the clumping of those episodes within an analysis window, while episode duration is only sensitive to the first. Three example activity patterns with the same total sleep duration but different sleep structures demonstrate some properties of these measures (Fig. 1).

Circadian and Environmental Regulation of Sleep Structure

In order to assess the usefulness of our approach to quantifying fly sleep structure, we analyzed sleep data acquired with the well-characterized *Drosophila* Activity Monitor (DAM) system (Trikinetics, Waltham, MA). Sleep in female wildtype (WT, *Canton Special*, n = 60) and circadian defective (*per*^{01} mutant, n = 57) flies was measured for 3 days in a 12:12 light:dark cycle (LD), after which the lights were set to off, and sleep was measured for 6 days in constant darkness (DD) (Fig. 2A-B). There is a significant main effect of day (ZT0-12) v. night (ZT12-24) and a significant interaction between time of day and genotype for all measures of sleep quantified (Repeated measures ANOVA; all $p < 0.0001$). Flies in DD without a functional circadian clock

212 produce identical sleep during the subjective day and night: the total duration, mean
213 episode duration, Hamming index, and probability of behavioral state transition do not
214 differ significantly (all $p > 0.3$; Fig. 2C-G). Light alone is a potent cue for differentiating
215 daytime and nighttime sleep. In *per*^{01} flies lacking an internal circadian clock, light
216 causes significant decreases in total sleep and mean episode duration, and significant
217 increases in Hamming index, P(Wake), and P(Doze) (all $p < 0.0001$; Fig. 2C-G). The
218 circadian clock also drives significant differences between daytime and nighttime sleep
219 in the absence of light. WT flies in DD conditions have less total sleep, higher Hamming
220 index, and a higher P(Wake) during subjective day than night (all $p < 0.0001$; Fig. 2C-
221 G). Mean sleep episode duration and P(Doze) are regulated by environmental light
222 alone (all $p < 0.0001$), but not by the circadian clock in DD (all $p > 0.06$; Fig. 2D,G).
223 Finally, when flies have two sources of information about time of day, both an LD cycle
224 and circadian clock, flies sleep more with longer mean episode duration at night (all $p <$
225 0.0001). However, sleep fragmentation as measured by Hamming Index, is significantly
226 higher at night than during the day ($p < 0.0001$). P(Wake) is significantly lower at night
227 in WT flies in LD ($p < 0.0001$), while P(Doze) is not significantly regulated by time of day
228 ($p = 0.067$).

229 These group comparisons lead to three overall conclusions. First, P(Wake) is
230 regulated more strongly by environmental light than by the circadian clock. This is
231 consistent with locomotor activity and deep sleep stages following the LD cycle rather
232 than the circadian cycle during forced desyncronization studies(Cambras et al., 2007;
233 José Chiesa et al., 2007). Second, P(Doze) is not strongly regulated by light or by the
234 circadian clock. This suggests that P(Wake) may be the major regulator of total sleep

and strongly influence mean episode duration. Lastly, the regulation of sleep fragmentation appears to be more complex than the regulation of total sleep.

In order test these group-level associations, we measured the strength of the relationships between the behavioral state transition probabilities P(Wake) and P(Doze), and measures of sleep structure (Table 1). Across conditions and genotypes, P(Wake) is strongly correlated with both total sleep and mean episode duration, but is not significantly correlated with Hamming Index. P(Doze) is moderately, but significantly, correlated with total sleep, mean episode duration, and Hamming Index. P(Wake) and P(Doze) are not correlated with one another. While these correlations are suggestive, they cannot unambiguously demonstrate causation, especially due to the complexity of sleep regulation in flies (Tomita et al., 2017). An *in silico* approach to sleep offers a more controlled arena in which to investigate the potential causal relationships among these behavioral parameters.

In Silico Sleep Recapitulates Features of In Vivo Fly Sleep

We used an agent-based simulation paradigm to generate *in silico* sleep data. Each *in silico* fly was initialized in a random state (either active or inactive) and with a P(Wake) and P(Doze). At each subsequent time step, the simulation used the current state of the fly and the behavioral transition probability to determine the new state of the fly. WT and per^{01} fly sleep data (from Fig. 2) were used to generate empirical heat maps of the relationship between P(Doze), P(Wake), and sleep parameters (Fig. 3A). Corresponding *in silico* sleep data was generated for each combination of P(Doze) and P(Wake) (range: 0-1 binned to 25 steps, n = 100 simulations per bin; Fig. 3B).

Comparison of the *in vivo* and *in silico* datasets shows qualitative similarity with some notable quantitative differences, especially in mean sleep episode duration (Fig. 3A,B, *middle column*). One possible explanation for this quantitative discrepancy is that our model of state transition probability is too simple. For example, previous reports have shown that sensory thresholds and neural activity change as a function of the duration that the fly has been asleep (Nitz et al., 2002; van Alphen et al., 2013; Yap et al., 2017). This is similar to the situation in humans, where transition models consider sleep sub-states (Perez-Atencio et al., 2018).

In order to integrate this information into our models, we calculated P(Wake) and P(Doze) as a function of behavioral state duration (Fig. 3C,D). We found both P(Wake) and P(Doze) have a power-law relationship with the duration of activity state. The power law relationship has three parameters: *a*, the intercept, *b*, the exponent, and *c*, the lower bound. Parameter *a* is the baseline transition probability of the fly. Parameter *b* is the rate at which the fly progresses from the behavioral transition into either deep sleep or full alertness. Parameter *c* is the long-term steady state behavioral transition probability in deep sleep or full alertness (Fig. 3C,D). We then used the values for P(Wake) and P(Doze), and the best-fit power-law functions, to generate new *in silico* data matched to LD day, LD night, DD day, and DD night in WT flies. We then compared the deviation of our simulations from the *in vivo* WT fly data (n = 100 *in silico* flies per condition; Fig. 3E). We refer to the simulations with a fixed P(Wake) and P(Doze) as “Markov Chain simulations,” because they are a special case of a Markov chain. Both the Markov chain and power law *in silico* flies accurately reproduce total sleep of their matched *in vivo* group (Fig. 3E, *left column*). The Markov chain simulations systematically underestimate

sleep episode duration, while the power law simulations match the *in vivo* data (Fig. 3E, *middle column*). Both the Markov and power law simulations produce higher Hamming index *in silico* sleep than the *in vivo* equivelent (Fig. 3E, *right column*). Across groups, the majority of both the Markov chain and power law simulations show small standardized differences from *in vivo* data (|*Z*-score| < 2), indicating that the relatively low complexity simulations are capable of capturing a meaningful fraction of the *in vivo* behavior.

Our simulation approach assumes that population-wide fit of behavioral state transition probability can be used to simulate *in silico* individuals. We tested the assumption that individual fly behavior is faithfully represented by population means using two approaches (Fig. 4). First, we tested the hypothesis that variation of a single fly's behavior over time is comparable to the variation in behavior between flies (Fig. 4A,B). We found instead that for both P(Wake) and P(Doze), there is significantly greater variability between flies than within a single fly across time (two tailed *T*-test; $p < 0.0001$). Second, we tested the hypothesis that estimates of P(Wake) and P(Doze) derived from each individual fly would converge toward the population estimate of these measures. Population estimates of P(Wake) and P(Doze) are centrally located within the distribution of individual fly derived estimates (Fig. 4C,D). Population estimates of the power law distribution parameters of P(Wake) and P(Doze) are also relatively faithfully reproduced by the distribution of individual fly estimates, with the notable exception of the lower-bound parameter of P(Wake) (Fig. 4E-J). In all individual flies, the lower bound of P(Wake) was estimated to be zero, while as a population the lower bound was 0.5% (Fig. 4I). This discrepancy is likely due to the difficulty of getting a

good estimate of low frequency events from limited data, and would be most apparent when estimating the frequency of long duration sleep episodes. While it is in principle possible to estimate the single fly P(Wake) and P(Doze), fitting a power law function to individual fly data is hampered by our inability to accurately assess long-duration episode frequency because data from any one animal is limited. The distribution of P(Wake) and P(Doze) and their power law fit parameters are unimodal, allowing population-based averages to approximate a “typical” fly.

Aging Alters Sleep Structure and Behavioral State Transition Probability

To test the utility of our analysis tools and investigate the relationship of these new metrics to specific biological processes, we applied them to data sets acquired under conditions known to significantly affect sleep. The total amount and structure of sleep produced by an individual is strongly regulated by age in many animals, including flies (Koh et al., 2006; Vienne et al., 2016). In groups of age-matched flies, probability of wake is the dominant factor in determining sleep amount and quality (Fig. 2). We measured sleep in aged flies in order to determine if P(Wake) also drives aging-related changes in sleep. Sleep was measured in cohorts of WT flies during week 1, 3, 5, and 7/8 post eclosion (n = 48, 30, 30, and 39, respectively; weeks 7 & 8 were combined due to a low rate of survival to this age). In agreement with prior results, we find that the 24 hour profile of sleep is altered in aged flies, most dramatically during the day (Fig. 5A). In these cohorts of flies, we found that old flies sleep significantly longer than young flies, but are hyperactive while awake ($p < 0.0002$; Fig. 5B,C). Mean sleep episode duration was not strongly affected by aging in this experiment; only the week 5 cohort

significantly differed from young flies in nighttime episode duration ($p = 0.0001$; Fig. 5D). However, there is a steady increase in daytime Hamming Index with age ($p < 0.0001$; Fig. 5E), in agreement with both the prior finding that sleep fragmentation increases with age (Koh et al., 2006; Vienne et al., 2016) and the altered circadian profile (Fig. 5A). Perhaps surprisingly given our results comparing groups of young flies (Fig. 2), nighttime P(Wake) does not vary significantly with age, and daytime P(Wake) is only significantly decreased in the oldest group of flies ($p < 0.0001$; Fig. 5F). In contrast, P(Doze) increases with age both during the day and night ($p < 0.0001$; Fig. 5G). We plotted the changes in P(Wake) and P(Doze) as a trajectory through a probability space in order to gain insight into how aging-related changes in behavioral transition probability are revealed in behavior (Fig. 5H). We can observe that nighttime behavior follows a linear path that falls within a high-sleep area of the probability space, consistent with the relatively modest changes in sleep quantity at night (Fig. 5A,B,H). The probability space occupied by nighttime sleep is also predicted to have low fragmentation (Fig. 3B), consistent with the low and relatively consistent Hamming Index of nighttime sleep across age. Daytime behavior follows a more complex path that moves from a low-sleep area of the space toward a high-sleep area (Fig. 5H) that is also a high fragmentation region (Fig. 3B). In this aging dataset, we find that both the changes in sleep quantity and structure are explained by changes in P(Wake) and P(Doze), and recapitulated in a simple Markov chain simulation.

Effect of Increased Homeostatic Sleep Pressure on Behavioral State Transitions

Sleep deprivation in flies, like in other animals, leads to increased subsequent sleep (Shaw et al., 2000). A common model for the generation of increased sleep after release from sleep deprivation posits that there is an increase in sleep “pressure” which alters sleep drive (Fuller et al., 2006). In order to quantify how sleep deprivation and homeostasis affects behavioral state transitions, we performed a sleep deprivation experiment during which WT flies were shaken periodically for 12 hours overnight (*n* = 120 shaken, 117 control; Fig. 6A). Compared with a control group of flies, flies that were shaken slept less while the shaker was on, and more the following day (Fig. 6A). We defined two time windows: PRE, ZT0-6 the morning prior to sleep deprivation, and POST, ZT0-6 the morning following sleep deprivation. Sleep deprived flies, but not control flies, slept significantly more POST than PRE and had significantly less sleep fragmentation as assessed both by Hamming Index (all $p < 0.0001$; Fig. 6B,C) and mean episode duration (in minutes, for shaken group, PRE = 40.9 (SD 44.4), POST = 206.8 (SD 137.9), $p < 0.0001$, for control group, PRE = 40.2 (SD 49.1), POST = 52.2 (SD 61.7), $p = 0.2$). P(Wake) was significantly decreased and P(Doze) was significantly increased in sleep deprived flies (all $p < 0.0001$), but not control flies, during the POST interval (Fig. 6D,E).

While both P(Wake) and P(Doze) are significantly different following sleep deprivation, three lines of evidence suggest that P(Wake) is principally responsible for homeostatic rebound sleep: 1) change in total sleep during POST v. PRE is more strongly correlated with change in P(Wake) ($R = -0.97$, $p < 0.0001$) than change in P(Doze) ($R = 0.19$, $p = 0.06$), 2) The effect size of the change in P(Wake) is larger than

the effect size of P(Doze) (Cohen's d = -1.46 and 0.81, respectively, (Cohen, 1992)) and 3) Superimposing the observed change in P(Wake) and P(Doze) on simulated data, the change along the P(Wake) axis is more consequential than the change along the P(Doze) axis (Fig. 6F,G). Examining the history-dependence of P(Wake) and P(Doze) provides additional insight into how sleep deprivation modifies behavioral transitions (Fig. 6H,I). Neither the initial value (PRE: 1.24 ± 0.08, POST:1.30 ± 0.06) nor the long-term lower bound of P(Wake) (PRE: 0, POST: 0) differs between PRE and POST, but the P(Wake) power law exponent (parameter *b*) is substantially larger in POST (PRE: 1.03 ± 0.04, POST: 1.20 ± 0.04; Fig. 6H).

In WT flies, it appears that the primary mechanism generating rebound sleep is a decreased probability of waking up during a sleep episode, not the initiation of additional episodes. The change in P(Wake) does not result from a change in the properties of deep sleep, but from the flies more rapidly entering deep sleep after initiating a sleep episode. It is clear from the heat maps (Fig. 6F,G), however, that if a fly's initial position (i.e. their respective P(Wake) and P(Doze)) was in the lowest left part of the map, the effect of changes in P(Doze) might be behaviorally relevant. The fact that both mechanisms can be engaged could be important in animals, e.g. mutants, whose initial sleep parameters are abnormal.

Mutations Affecting Sleep Act Through Both Wake and Doze Probability

Sleep is regulated by a multitude of molecular processes, and many null and hypomorphic mutations disrupt sleep in flies (Helfrich-Förster, 2018). We examined how two known sleep mutants, *fumin* (dat^{fmn}; n = 37 male flies; Kume et al., 2005) and

insomniac (*inc*^{2}; n = 31; Stavropoulos and Young, 2011), affect behavioral state transition probabilities (Fig. 7). We found that both *fumin* and *insomniac* flies have decreased total sleep relative to control flies with the same genetic background (*w*^{1118}; *n* = 40; $p < 0.0001$; Fig.6A,B). In addition to sleeping less, *fumin* flies are significantly hyperactive when awake during the day ($p = 0.0005$; Fig. 7C). *Fumin* and *insomniac* flies have significantly reduced mean sleep episode durations both during the day and night ($p < 0.0001$; Fig. 7D). During the day both *fumin* and *insomniac* flies have significantly elevated Hamming fragmentation ($p = 0.012$), while only *insomniac* flies have significantly more fragmented sleep at night by this metric ($p < 0.0001$). Visual examination of individual sleep rasters confirms that despite having shorter mean sleep episodes, nighttime sleep and activity in *fumin* flies is not dramatically more disorganized than in wild type (Fig. S1). In summary, both *fumin* and *insomniac* flies sleep less than WT and in shorter episodes both during the day and night. *Fumin* flies have a more severe total sleep phenotype, *insomniac* flies have a more severe sleep fragmentation phenotype.

Both the *fumin* and *insomniac* phenotypes can be explained by changes in P(Wake) and P(Doze) (Fig. 7F-G). *Fumin* flies have increased P(Wake) both during the day and the night ($p < 0.0001$), which our simulations predict would cause the observed phenotypes (Fig. 7H,I). The *insomniac* mutation results in significantly increased P(Wake), and also increases P(Doze), both during the day and night ($p < 0.0001$). Using the simulation-based maps of total sleep and Hamming index as functions of P(Wake) and P(Doze), we find that the changes in sleep behavior observed in *in vivo* flies are recapitulated *in silico* (Fig. 7H,I). The power law functions of P(Wake) and

P(Doze) provide additional insight into this process (Fig. 7J,K). The increase in P(Wake) between WT and *fumin* flies is driven by a difference between the respective power law exponents of decay (WT: 1.24 ± 0.07, *fumin*: 0.88 ± 0.05) as there is not a significant difference between the initial values of P(Wake) for the genotypes (WT: 1.18 ± 0.08, *fumin*: 1.04 ± 0.10; Fig. 7H). The increase in P(Doze) between WT and *insomniac* flies is driven by differences in the initial value of P(Doze) (WT: 0.46 ± 0.09, *insomniac*: 1.42 ± 0.29) as *insomniac* flies have a slightly elevated exponent of decay (WT: 0.56 ± 0.09, *insomniac*: 0.88 ± 0.12; Fig. 7I). The divergent effects of these two mutations, while complex, are well explained by a relatively simple model of behavioral state transition probability.

DISCUSSSION

Sleep serves many physiological purposes, so it is unsurprising that it should be responsive to many different variables. Competing or interacting switches which are organized hierarchically can allow many factors to be integrated. Succinctly expressing the global state of such a complex system requires finding a level of abstraction that is both comprehensible and biologically-based. In this paper we address this problem by measuring and modeling sleep in terms of the probability of wake/sleep transitions. We also introduce a new measure of sleep fragmentation, the Hamming Index, which gives a quantitative assessment of the organization of the sleep episodes in the epoch being studied.

Sleep is a Probabilistic Behavior

Sleep as a probabilistic behavior has been extensively modelled in both rodents and humans (Bianchi et al., 2012; Perez-Atencio et al., 2018; Stephenson et al., 2016; Yang and Hursch, 1973). Previous descriptions of *Drosophila* sleep structure have focused on describing the relative frequency of sleep episodes of different durations (Diamond, 2016; Ueno et al., 2012). These reports each found that fly sleep follows a power-law distribution of sleep episode duration, and that the distribution is affected by a variety of factors, including environment and dopamine levels. Each report also suggested a metric for quantifying sleep structure: coefficient of determination (Diamond, 2016), or power-law fit coefficients (Ueno et al., 2012). This report both agrees with and builds upon this previous work. We find that P(Wake) is strongly correlated with mean episode duration and that both P(Wake) and P(Doze) follow a power-law dependence upon duration of sleep and wake, respectively (Table 1, Fig. 3). We also find that dopamine profoundly affects P(Wake), consistent with a shift in the distribution of episode duration (Ueno et al., 2012). By focusing not on sleep episodes themselves, but on the state transitions that define sleep episodes, we also gain insight into the mechanisms that generate the observed distribution of sleep episode duration. This mechanistic advantage is most apparent in the comparison of biological data to *in silico* data for a wide range of conditional probabilities (Fig. 3), which allows us to plot the positions of flies in a conditional probability space.

Probability of Wake is a Measure of Sleep Depth

Sleep is a behavior in which movement and responses to external stimuli are suppressed. The more strongly these properties are expressed, the “deeper” sleep is considered to be. In humans, sleep depth is measured based on vital signs, EEG, and behavior, which together provide a holistic view of sleep depth (Bonnet et al., 2007). Sleep depth in flies is more difficult to characterize. Total LFP power in flies is significantly reduced immediately after the initiation of sleep, and does not decrease further to indicate sleep depth (van Alphen et al., 2013). Because of the limited information about sleep and technical complexity of measuring LFP, sleep depth is most commonly measured in flies using arousal threshold (Guo et al., 2011; Huber et al., 2004; Linford et al., 2012; Shaw et al., 2000; van Alphen et al., 2013). Arousal threshold increases during early sleep and reaches a local maximum at approximately 10-15 minutes (Huber et al., 2004; van Alphen et al., 2013). Measuring arousal threshold requires waking the flies and interrupting sleep in progress, which has two experimental implications. First, repeatedly probing a single group of flies disrupts the normal progression of sleep, so collecting a time-course of sleep depth requires either significantly over-sampling a random stimulus or measuring many groups of flies. Second, measuring arousal threshold perturbs any subsequent sleep-dependent process, confounding measurements of the link between sleep depth and other behaviors, such as courtship or learning.

In light of the limitations of arousal threshold, probability of spontaneous awakening, or P(Wake), is an attractive measure of sleep depth. The likelihood of waking up is logically linked to the depth of sleep, and several lines of evidence

reinforce the face-plausibility. First, spontaneous self-awakenings are less likely during deeper sleep stages in humans (Zepelin, 1986). Second, the *fumin* mutation, which has been previously described as an arousal-threshold mutation (Kume et al., 2005), strongly regulates P(Wake) and only weakly affects P(Doze). Third, the time course of P(Wake) decreasing and arousal threshold increasing after the initiation of sleep is similar (Huber et al., 2004; van Alphen et al., 2013). Fourth, P(Wake) is a strong predictor of sleep episode duration (Table 1), and sleep episode duration and arousal threshold co-vary (Guo et al., 2011; Linford et al., 2012). In light of this evidence, we propose that P(Wake) is a behavioral correlate of sleep depth in flies.

Probability of Doze is a Measure of Sleep Pressure

After long periods of wake, the desire to sleep also increases. This homeostasis-promoting desire to sleep is described as “sleep pressure,” or process S, in the influential Borbely two-factor model of sleep (Borbély, 1982). Sleep pressure is difficult to measure directly because it is an internal state rather than an external behavior. The most common measure of sleep pressure is change in total sleep, *i.e.* rebound sleep (Huber et al., 2004). However, total sleep is inevitably confounded by sleep depth, potentially masking the effects of sleep pressure. Another common measure of sleep pressure is the latency to sleep after an environmental cue, such as lights turning off (Andretic and Shaw, 2005). Sleep latency is not confounded by sleep depth, but it can only be measured relative to a pre-defined marker, and only once per fly per event.

Probability of doze, P(Doze), is conceptually similar to sleep latency. The primary difference between the two measures is that sleep latency is measured against an

external time marker, while P(Doze) is measured against fly-initiated movement. Due to this similarity in calculation, we expected that P(Doze) would measure a similar biological process to sleep latency, namely sleep pressure. Empirically, we find that P(Doze) behaves as we would expect a measure of sleep pressure to behave. First, P(Doze) is not strongly regulated by the circadian clock, consistent with Borbély's process "S" being non-circadian (Borbély, 1982). Second, P(Doze) is also not a major determinant of total sleep in un-manipulated flies, consistent with inhibiting the sleep homeostat having only a minimal effect on baseline sleep (Liu et al., 2016). Third, the drive to sleep and the maintenance of sleep are separate processes in flies (Agosto et al., 2008), and P(Doze) and P(Wake) are not significantly correlated with one another. Finally, P(Doze) is increased by sleep deprivation, consistent with a homeostatic pressure process. We note that while the regulation of P(Doze) by sleep deprivation is significant, changes in P(Wake) co-occur and that the P(Wake) effect is the primary driver of rebound sleep in wild type flies (Fig. 6). The indirect role of sleep pressure in generating rebound sleep may give additional insight into the privileged roles of some neural circuits in increasing total sleep after sleep deprivation (Seidner et al., 2015).

Counter-intuitively for a measure of sleep pressure, P(Doze) is correlated with increased sleep fragmentation (Table 1). P(Doze) is the probability of initiating sleep episodes, and the median sleep episode is shorter than the mean episode (Diamond, 2016), so it follows that increasing P(Doze) will usually result in shorter mean sleep episode duration. The implication of this finding is that sleep fragmentation is not, on its own, evidence of a wake-promoting process. Our results indicate that fragmented sleep

can be the result of decreased sleep depth (*i.e.* high P(Wake)), increased sleep pressure (*i.e.* high P(Doze)), or a combination of the two.

Hamming Index is a Robust Measure of Sleep Fragmentation

Fragmentation of sleep is a critical human health issue, and the major way that this is assessed in patient populations is by use of measures analogous to sleep bout duration (sleep stage percentages and sleep efficacy) from polysomnography records (Costello et al., 2014). These methods, however, can fail to capture fragmentation even in patients with obstructive sleep apnea (Swihart et al., 2008). Models that extract information about transitions and the underlying organization of episodes have been shown to be better predictors of fragmentation and morbidity (Bianchi et al., 2010; Bianchi et al., 2012; Swihart et al., 2008). For *Drosophila* sleep the episode duration serves as the major metric for fragmentation. Episode duration, however, can fail to identify changes in consolidation. For example in wildtype animals in DD there is no difference between episode duration in subjective day and night, but there are clock-dependent processes consolidating sleep that can be detected in the Hamming Index (Fig. 2). Hamming Index also performs much better than mean episode duration in detecting age-induced sleep fragmentation (Fig. 5).

Sleep Pressure and Sleep Depth are Regulated by Diverse Processes in Flies

The utility of these new analysis tools is demonstrated by the deeper level of insight gained by examining well-studied manipulations of fly sleep. In wild type and clockless (per^{01}) mutants, we found that most of the difference between day and night

sleep can be attributed to changes in sleep depth, not sleep pressure. Aged flies have been reported to have more fragmented sleep (Koh et al., 2006; Vienne et al., 2016), a finding we can reproduce using the Hamming Index. We find that aging results in orthogonal changes in sleep pressure and sleep depth that move the flies through the transition probability space in an orderly manner, with a consistent increase in sleep pressure with increasing age, and an inverted-U curve of sleep depth with development and aging. Mechanical sleep deprivation of wild type flies results in increase sleep pressure and sleep depth following release from deprivation. The quantity of homeostatic rebound sleep, like normal sleep, appears to be controlled primarily by sleep depth, not by sleep pressure directly. Regulation of sleep pressure and sleep depth is genetically separable, as we found that the short sleep mutant *fumin* only affects sleep depth, while *insomniac* significantly alters both sleep pressure and sleep depth. Despite the similarities in these two alleles at the level of total sleep, the underlying molecular and circuit processes they affect must be different.

Conclusions

In this report, we treat sleep and wake as binary behavioral states and measure the probability that animals transition between them. This is a dramatic simplification of sleep and waking behavior, but even so, it is sufficient to capture an interesting fraction of the behavioral variability between flies responding to perturbation. Classifying behavior into discrete states to determine transition probabilities and pathways is an approach that has been applied to many behaviors, including swimming (Willows and Hoyle, 1969), grooming (Berridge et al., 1987), feeding (Martaresche et al., 2000), and

navigation (Hernandez-Nunez et al., 2015; Kato et al., 2015). The possible scope of this type of analysis is rapidly expanding due to the increasing sophistication of machine vision hardware and software, which greatly facilitate unbiased and high-throughput classification of behavior (Hong et al., 2015; Kabra et al., 2013; Mirat et al., 2013; van den Boom et al., 2017). Correlation of behavioral transition probabilities with behavioral drives and covert states, as we have done with *Drosophila* sleep, may provide additional insight in these freshly accessible contexts.

LITERATURE CITED

Agosto, J., Choi, J. C., Parisky, K. M., Stilwell, G., Rosbash, M. and Griffith, L. C. (2008). Modulation of GABAA receptor desensitization uncouples sleep onset and maintenance in Drosophila. *Nat. Neurosci.* **11**, 354–9.

Andretic, R. and Shaw, P. J. (2005). Essentials of Sleep Recordings in Drosophila: Moving Beyond Sleep Time. In *Methods in enzymology*, pp. 759–772.

Andretic, R., van Swinderen, B. and Greenspan, R. J. (2005). Dopaminergic modulation of arousal in Drosophila. *Curr. Biol.* **15**, 1165–75.

Baud, M. O., Magistretti, P. J. and Petit, J.-M. (2013). Sustained sleep fragmentation affects brain temperature, food intake and glucose tolerance in mice. *J. Sleep Res.* **22**, 3–12.

Berridge, K. C., Fentress, J. C. and Parr, H. (1987). Natural syntax rules control action sequence of rats. *Behav. Brain Res.* **23**, 59–68.

Berry, J. A., Cervantes-Sandoval, I., Chakraborty, M. and Davis, R. L. (2015). Sleep Facilitates Memory by Blocking Dopamine Neuron-Mediated Forgetting. *Cell* **161**, 1656–67.

Bianchi, M. T., Cash, S. S., Mietus, J., Peng, C.-K. and Thomas, R. (2010). Obstructive Sleep Apnea Alters Sleep Stage Transition Dynamics. *PLoS One* **5**, e11356.

Bianchi, M. T., Eiseman, N. A., Cash, S. S., Mietus, J., Peng, C.-K. and Thomas, R. J. (2012). Probabilistic sleep architecture models in patients with and without sleep apnea. *J. Sleep Res.* **21**, 330–341.

Bonnet, M. H., Doghramji, K., Roehrs, T., Stepanski, E. J., Sheldon, S. H., Walters,

A. S., Wise, M. and Chesson, A. L. (2007). The scoring of arousal in sleep: reliability, validity, and alternatives. *J. Clin. Sleep Med.* **3**, 133–45.

Borbély, A. A. (1982). A two process model of sleep regulation. *Hum. Neurobiol.* **1**, 195–204.

Cambras, T., Weller, J. R., Anglès-Pujoràs, M., Lee, M. L., Christopher, A., Díez-Noguera, A., Krueger, J. M. and de la Iglesia, H. O. (2007). Circadian desynchronization of core body temperature and sleep stages in the rat. *Proc. Natl. Acad. Sci. U. S. A.* **104**, 7634–9.

Cohen, J. (1992). Statistical Power Analysis. *Curr. Dir. Psychol. Sci.* **1**, 98–101.

Costello, R. B., Lentino, C. V, Boyd, C. C., O'Connell, M. L., Crawford, C. C., Sprengel, M. L. and Deuster, P. A. (2014). The effectiveness of melatonin for promoting healthy sleep: a rapid evidence assessment of the literature. *Nutr. J.* **13**, 106.

Diamond, J. M. (2016). Goodness of fit to a mathematical model for Drosophila sleep behavior is reduced in hyposomnolent mutants. *PeerJ* **4**, e1533.

Donlea, J. M., Thimgan, M. S., Suzuki, Y., Gottschalk, L. and Shaw, P. J. (2011). Inducing sleep by remote control facilitates memory consolidation in Drosophila. *Science* **332**, 1571–6.

Eban-Rothschild, A. and Bloch, G. (2012). Social Influences on Circadian Rhythms and Sleep in Insects. *Adv. Genet.* **77**, 1–32.

Fuller, P. M., Gooley, J. J. and Saper, C. B. (2006). Neurobiology of the Sleep-Wake Cycle: Sleep Architecture, Circadian Regulation, and Regulatory Feedback. *J. Biol. Rhythms* **21**, 482–493.

Guo, F., Yi, W., Zhou, M. and Guo, A. (2011). Go signaling in mushroom bodies regulates sleep in Drosophila. *Sleep* **34**, 273–81.

Hamming, R. W. (1950). Error Detecting and Error Correcting Codes. *Bell Syst. Tech. J.* **29**, 147–160.

Helfrich-Förster, C. (2018). Sleep in Insects. *Annu. Rev. Entomol.* **63**, 69–86.

Hernandez-Nunez, L., Belina, J., Klein, M., Si, G., Claus, L., Carlson, J. R. and Samuel, A. D. (2015). Reverse-correlation analysis of navigation dynamics in Drosophila larva using optogenetics. *Elife* **4**, e06225.

Hong, W., Kennedy, A., Burgos-Artizzu, X. P., Zelikowsky, M., Navonne, S. G., Perona, P. and Anderson, D. J. (2015). Automated measurement of mouse social behaviors using depth sensing, video tracking, and machine learning. *Proc. Natl. Acad. Sci.* **112**, E5351–E5360.

Huber, R., Hill, S. L., Holladay, C., Biesiadecki, M., Tononi, G. and Cirelli, C. (2004). Sleep homeostasis in Drosophila melanogaster. *Sleep* **27**, 628–39.

José Chiesa, J., Díez-Noguera, A. and Cambras, T. (2007). Effects of Transient and Continuous Wheel Running Activity on the Upper and Lower Limits of Entrainment to Light-Dark Cycles in Female Hamsters. *Chronobiol. Int.* **24**, 215–234.

Kabra, M., Robie, A. A., Rivera-Alba, M., Branson, S. and Branson, K. (2013). JAABA: interactive machine learning for automatic annotation of animal behavior. *Nat. Methods* **10**, 64–67.

Kato, S., Kaplan, H. S., Schrödel, T., Skora, S., Lindsay, T. H., Yemini, E., Lockery, S. and Zimmer, M. (2015). Global Brain Dynamics Embed the Motor Command Sequence of Caenorhabditis elegans. *Cell* **163**, 656–669.

Koh, K., Evans, J. M., Hendricks, J. C. and Sehgal, A. (2006). A Drosophila model for age-associated changes in sleep:wake cycles. *Proc. Natl. Acad. Sci. U. S. A.* **103**, 13843–7.

Kume, K., Kume, S., Park, S. K., Hirsh, J. and Jackson, F. R. (2005). Dopamine is a regulator of arousal in the fruit fly. *J. Neurosci.* **25**, 7377–84.

Lim, A. S. P., Yu, L., Costa, M. D., Leurgans, S. E., Buchman, A. S., Bennett, D. A. and Saper, C. B. (2012). Increased Fragmentation of Rest-Activity Patterns Is Associated With a Characteristic Pattern of Cognitive Impairment in Older Individuals. *Sleep* **35**, 633–640.

Linford, N. J., Chan, T. P. and Pletcher, S. D. (2012). Re-patterning sleep architecture in Drosophila through gustatory perception and nutritional quality. *PLoS Genet.* **8**, e1002668.

Liu, S., Liu, Q., Tabuchi, M. and Wu, M. N. (2016). Sleep Drive Is Encoded by Neural Plastic Changes in a Dedicated Circuit. *Cell* **165**, 1347–1360.

Martaresche, M., Le Fur, C., Magnusson, M., Faure, J. M. and Picard, M. (2000). Time structure of behavioral patterns related to feed pecking in chicks. *Physiol. Behav.* **70**, 443–51.

Martin, M. Saint, Sforza, E., Crawford-Achour, E., Pascal, L., Lienard, G. and Frédéric, R. (2016). Sleep breathing disorders and cognitive decline in healthy elderly followed for eight years: The PROOF cohort. *Ann. Phys. Rehabil. Med.* **59**, e99.

Mirat, O., Sternberg, J. R., Severi, K. E. and Wyart, C. (2013). ZebraZoom: an automated program for high-throughput behavioral analysis and categorization.

Front. Neural Circuits **7**, 107.

Nitz, D. A., van Swinderen, B., Tononi, G. and Greenspan, R. J. (2002). Electrophysiological correlates of rest and activity in Drosophila melanogaster. *Curr. Biol.* **12**, 1934–40.

Perez-Atencio, L., Garcia-Aracil, N., Fernandez, E., Barrio, L. C. and Barios, J. A. (2018). A four-state Markov model of sleep-wakefulness dynamics along light/dark cycle in mice. *PLoS One* **13**, e0189931.

Qian, Y., Yi, H., Zou, J., Meng, L., Tang, X., Zhu, H., Yu, D., Zhou, H., Su, K., Guan, J., et al. (2016). Independent Association between Sleep Fragmentation and Dyslipidemia in Patients with Obstructive Sleep Apnea. *Sci. Rep.* **6**, 26089.

Scammell, T. E., Arrigoni, E. and Lipton, J. O. (2017). Neural Circuitry of Wakefulness and Sleep. *Neuron* **93**, 747–765.

Seidner, G., Robinson, J. E., Wu, M., Worden, K., Masek, P., Roberts, S. W., Keene, A. C. and Joiner, W. J. (2015). Identification of Neurons with a Privileged Role in Sleep Homeostasis in Drosophila melanogaster. *Curr. Biol.* **25**, 2928–2938.

Shaw, P. J., Cirelli, C., Greenspan, R. J. and Tononi, G. (2000). Correlates of sleep and waking in Drosophila melanogaster. *Science* **287**, 1834–7.

Stavropoulos, N. and Young, M. W. (2011). insomniac and Cullin-3 regulate sleep and wakefulness in Drosophila. *Neuron* **72**, 964–76.

Stephenson, R., Caron, A. M. and Famina, S. (2016). Significance of the zero sum principle for circadian, homeostatic and allostatic regulation of sleep-wake state in the rat. *Physiol. Behav.* **167**, 35–48.

Swihart, B. J., Caffo, B., Bandeen-Roche, K. and Punjabi, N. M. (2008).

Characterizing sleep structure using the hypnogram. *J. Clin. Sleep Med.* **4**, 349–55.

Tomita, J., Ban, G. and Kume, K. (2017). Genes and neural circuits for sleep of the fruit fly. *Neurosci. Res.* **118**, 82–91.

Ueno, T., Masuda, N., Kume, S. and Kume, K. (2012). Dopamine modulates the rest period length without perturbation of its power law distribution in Drosophila melanogaster. *PLoS One* **7**, e32007.

van Alphen, B., Yap, M. H. W., Kirszenblat, L., Kottler, B. and van Swinderen, B. (2013). A dynamic deep sleep stage in Drosophila. *J. Neurosci.* **33**, 6917–27.

van den Boom, B. J. G., Pavlidi, P., Wolf, C. J. H., Mooij, A. H. and Willuhn, I. (2017). Automated classification of self-grooming in mice using open-source software. *J. Neurosci. Methods* **289**, 48–56.

Vienne, J., Spann, R., Guo, F. and Rosbash, M. (2016). Age-Related Reduction of Recovery Sleep and Arousal Threshold in Drosophila. *Sleep* **39**, 1613–24.

von Economo, C. (1930). Sleep as a problem of localization. *J. Nerv. Ment. Dis.* **71**, 249–259.

Willows, A. O. and Hoyle, G. (1969). Neuronal network triggering a fixed action pattern. *Science* **166**, 1549–51.

Yang, M. C. and Hursch, C. J. (1973). The use of a semi-Markov model for describing sleep patterns. *Biometrics* **29**, 667–76.

Yap, M. H. W., Grabowska, M. J., Rohrscheib, C., Jeans, R., Troup, M., Paulk, A. C., van Alphen, B., Shaw, P. J. and van Swinderen, B. (2017). Oscillatory brain activity in spontaneous and induced sleep stages in flies. *Nat. Commun.* **8**, 1815.

Zepelin, H. (1986). REM sleep and the timing of self-awakenings. *Bull. Psychon. Soc.*

24, 254–256.

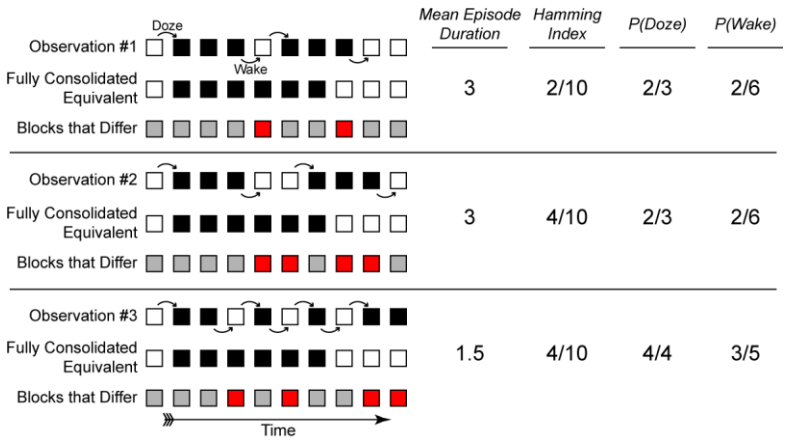

Figure 1 – Conditional Probability and Information Theory Measures of Sleep. Three exemplar sleep patterns (Observation #1-3) are shown that have the same total sleep and median time of sleep, but different structure. White squares: wake, Black squares: sleep. The minimum-distance, fully consolidated equivalent of each of these observations is the same (middle rows). During the calculation of Hamming Index, the Hamming distance to all possible fully consolidated equivalents is calculated to find the minimum value. Blocks that differ between each observation and the fully consolidated equivalent are red, blocks that are the same are gray. Transitions between behavioral states are indicated by curved arrows. Transitions from active to inactive (Doze) are above the blocks, transitions from inactive to active (Wake) are below. The calculation for P(Wake) is as follows: Count every measurement bin where the fly does not move except the last one. This the total number of transitions *from* inactive. For every measurement bin where the fly does not move, count the number where the fly moves at the next bin. This is the number of transitions *from* inactive *to* active. Divide the transitions *from* inactive *to* active by the total number of transitions to calculate the transition probability of inactive to active, or P(Wake). The calculation for P(Doze)

proceeds in the same way, but with “active” and “inactive” switched. See *Experimental Procedures* for additional details.

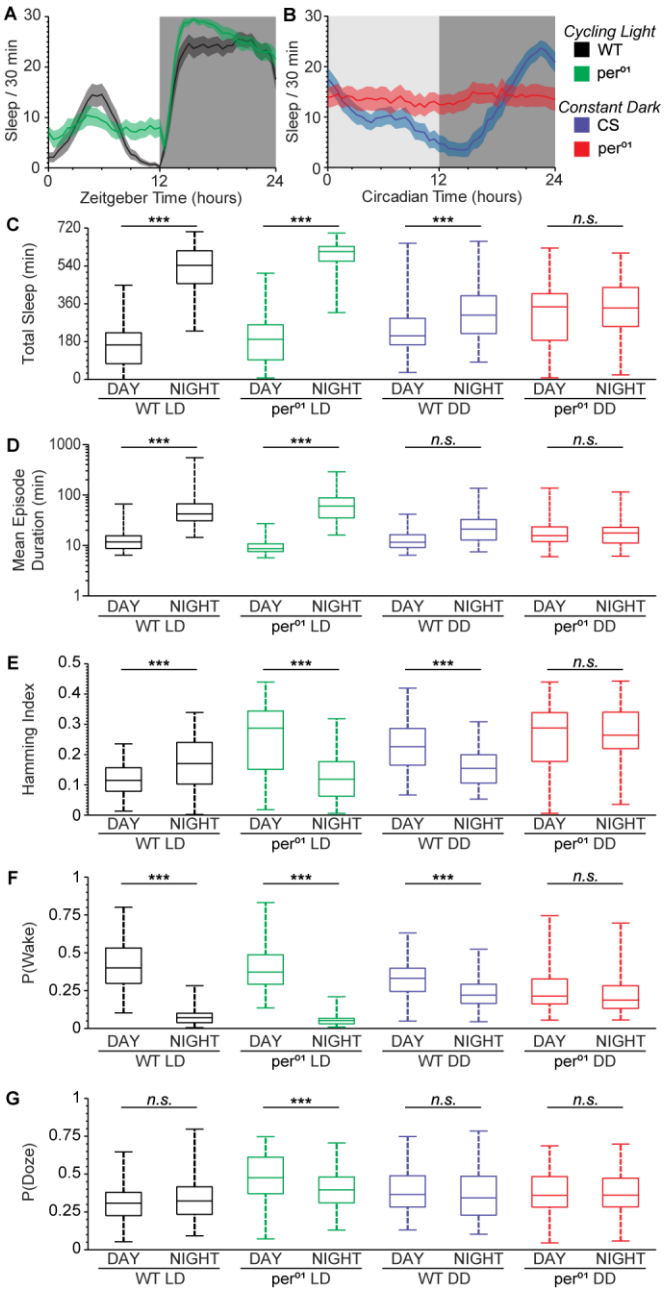

Figure 2 – Circadian and Environmental Regulation of Sleep Structure. (A-B) Circadian profile of sleep in a 12:12 Light:Dark cycle (LD; A) and in constant darkness (DD; B). Shaded regions indicate lights on and lights off times (A) or subjective day and night (B). Lines are the population average, shaded area is the 95% confidence interval of the mean. Individual profiles are the average of 3 days of behavior. DD sleep

measured on days 4-6 of constant darkness. (C-G) Box and whisker plots of total sleep (C), mean sleep episode duration (D), Hamming index (E), P(Wake) (F), and P(Doze) (G). Boxes show the 25/50/75th percentiles for each group, whiskers indicate the minimum and maximum. *n.s.* indicates no significant difference, * $p < 0.05$, ** $p < 0.005$, *** $p < 0.0005$.

TABLE 1 – Spearman Correlations Among Sleep Measures

	P(Wake) Rho	P(Wake) p-value	P(Doze) Rho	P(Doze) p-value
Total Sleep	-0.98	$< 10^{-10}$	0.22	1.2×10^{-6}
Mean Episode Duration	-0.89	$< 10^{-10}$	-0.16	5.7×10^{-4}
Hamming Index	-0.025	0.59	0.47	$< 10^{-10}$
P(Doze)	-0.077	0.096		

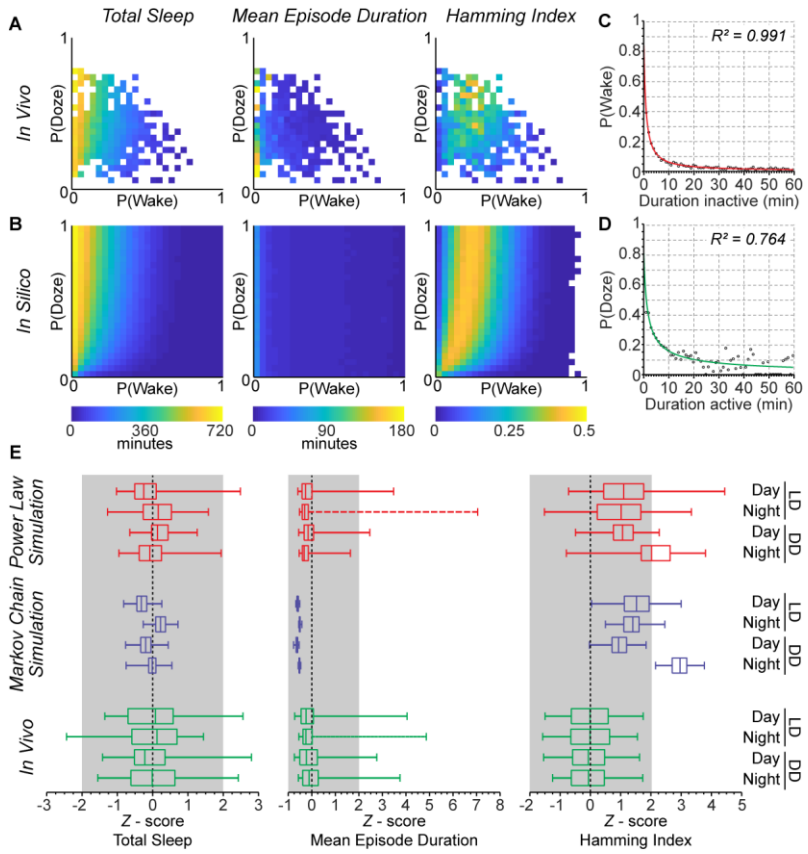

Figure 3 – *In Silico* Sleep Recapitulates Features of *In Vivo* Fly Sleep. (A, B) Heatmaps of *in vivo* (A) and *in silico* (B) sleep properties. (A) Each *In vivo* fly was assigned to one of 25 bins from 0 to 1 based upon it's respective P(Doze) and P(Wake). The mean value of total sleep (*left*), mean sleep episode duration (*center*), and Hamming index (*right*) was calculated for all samples in the bin, and the bin was assigned a color according to the legend (*bottom*). Coordinates without any samples are displayed as white. (B) For the central value of each P(Doze) and P(Wake) bin, 100 *in silico* flies were simulated. The mean value of each parameter of these simulations is displayed using the same color map as the *in vivo* data. Coordinates coded white for *in silico* Hamming index have an undefined value because no behavioral transitions were generated for the duration of the epoch. (C, D) P(Wake) and P(Doze) plotted as a function of the duration of inactivity (C) and activity (D), respectively. These data are

derived from the night epoch of CS flies in LD conditions. Data was fit using the equation $f(x) = a(x + 1)^{-b} + c$, where x is behavioral state duration and *a*, *b*, and *c* are free parameters. Black points are experimental data, red and green lines are the power law functions that best fit the data. (E) *Z*-scores of *in vivo* and *in silico* sleep. The population-derived values of P(Doze) and P(Wake), and their power-law equivalents, were derived for each listed *in vivo* experimental condition and used to simulate sleep behavior. *Z*-scores were calculated using the sample mean and standard deviation of the corresponding *in vivo* experimental group.

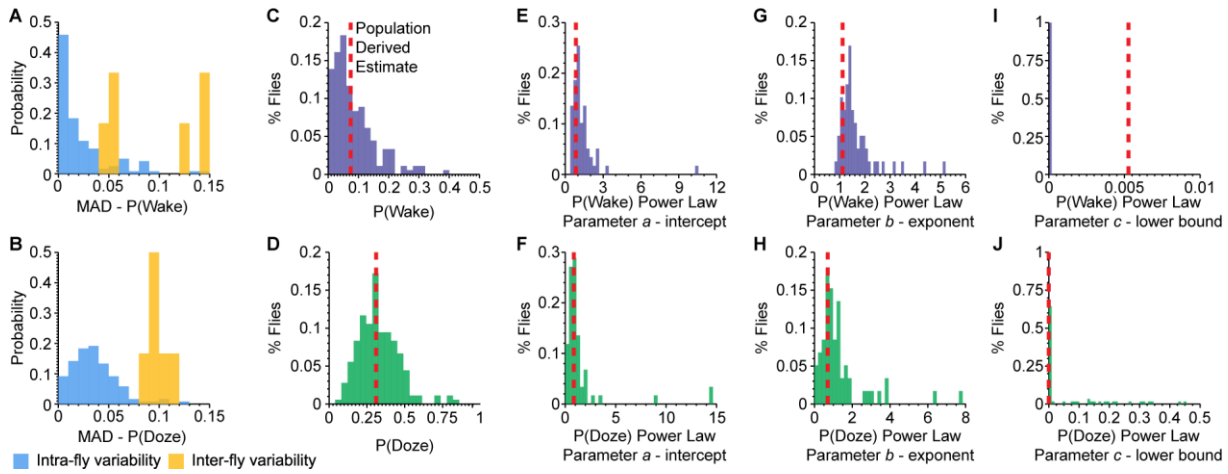

Figure 4 – Population and Individually Derived Estimates of Behavioral State Transition Probability. (A, B) Histograms of median absolute deviation (MAD) of P(Wake) (A) and P(Doze) (B). Intra-fly variability is calculated based on 3 day epochs and 3 night epochs of behavior from each fly. Inter-fly variability is based on the MAD of the population during each epoch (*n* = 60 WT flies). Low sample size of inter-fly variability in (A) precludes concluding if the data are bimodally distributed. (C, D) Histograms of P(Wake) and P(Doze) calculated for each fly. The population derived estimate is shown as a dashed red line. (E-J) Histograms of the estimates of each parameter, *a, b,* and *c*, of a power law fit using the equation $f(x) = a(x + 1)^{-b} + c$ of individual fly behavior. Data in (E-J) are from the nighttime behavior of CS flies in LD conditions.

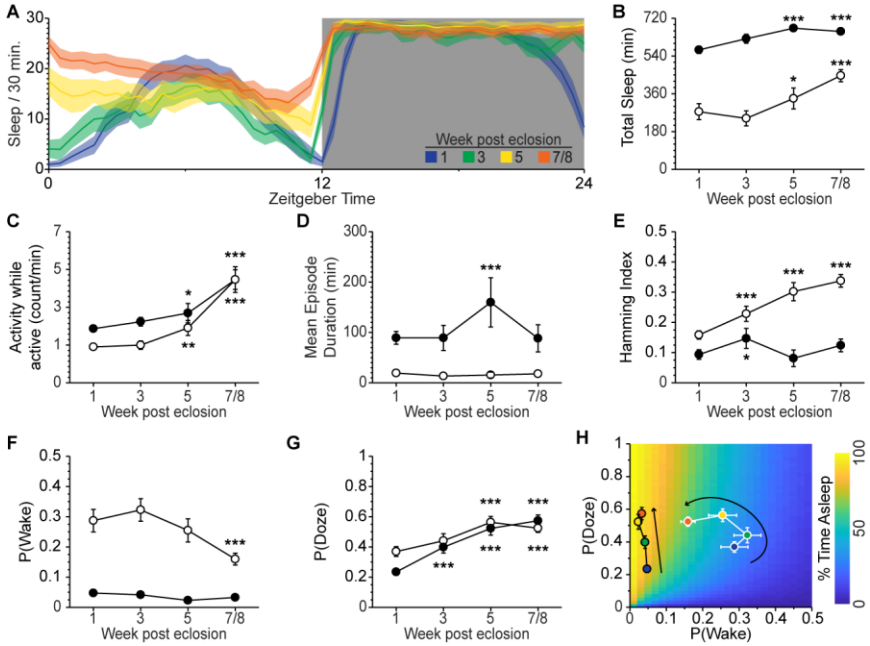

Figure 5 – Aging Alters Sleep Structure and Behavioral State Transition Probability. (A) Circadian profile of sleep of flies in their first (blue), third (green), fifth (yellow), or seventh/eighth (orange) week post-eclosion. Lines are the population average, shaded area is the 95% confidence interval of the mean. Individual profiles are the average of 3 days of behavior. (B-G) Mean and 95% confidence interval of total sleep (B), activity while active (C), mean sleep episode duration (D), Hamming index (E), P(Wake) (F), and P(Doze) (G). Daytime behavior: open circles, Nighttime behavior: filled circles. Significance is a corrected t-test vs. the week 1 value for each measure. (H) Trajectory of the flies over time along the P(Wake) and P(Doze) axes. Daytime trajectory: white outlines, Nighttime trajectory: black outlines. Error bars are 95% confidence intervals. Each point is color coded using the same scheme as the circadian profiles in (A). Arrows indicate the direction of increasing age. The background heatmap indicates the percent time asleep of Markov chain simulations calculated identically to

Figure 3B, but with finer binning resolution (mean of *n* = 100 simulations per bin). * $p < 0.05$, ** $p < 0.005$, *** $p < 0.0005$.

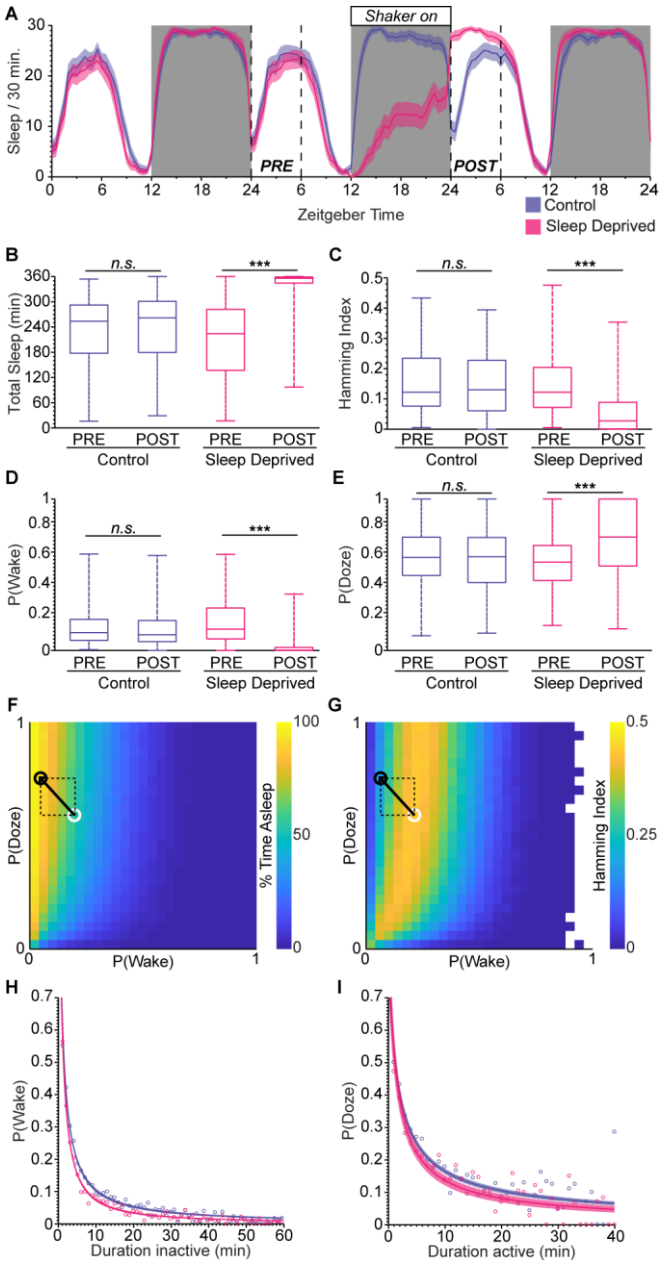

Figure 6 - Effect of Increased Homeostatic Sleep Pressure on Behavioral State Transitions. (A) Circadian profile of sleep over 3 days, including one night of sleep deprivation (labeled “Shaker on”). Shaded regions indicate lights on and lights off times. Analysis windows for PRE and POST are indicated. Mean sleep is indicated by lines, shaded region is the 95% confidence interval. (B-E) Box and whisker plots of total sleep (B), Hamming index (C), P(Wake) (D), and P(Doze) (E). Boxes indicate the 25/50/75th

percentiles for each group, whiskers indicate the minimum and maximum. (F,G) Heatmaps of simulated sleep at each level of P(Wake) and P(Doze), reproduced from Fig. 3. Circles indicate the coordinates of the mean P(Wake) and P(Doze) of sleep deprivation group before sleep deprivation (white circles) and following sleep deprivation (black circles). Dashed lines show the change along each dimension. (H,I) Power law function fits of P(Wake) and P(Doze) during PRE and POST. PRE: blue, POST: magenta. Open circles are the empirical data, lines are the best fit, and shaded regions are the 95% prediction bounds for the fit. *n.s.* indicates no significant difference, * $p < 0.05$, ** $p < 0.005$, *** $p < 0.0005$.

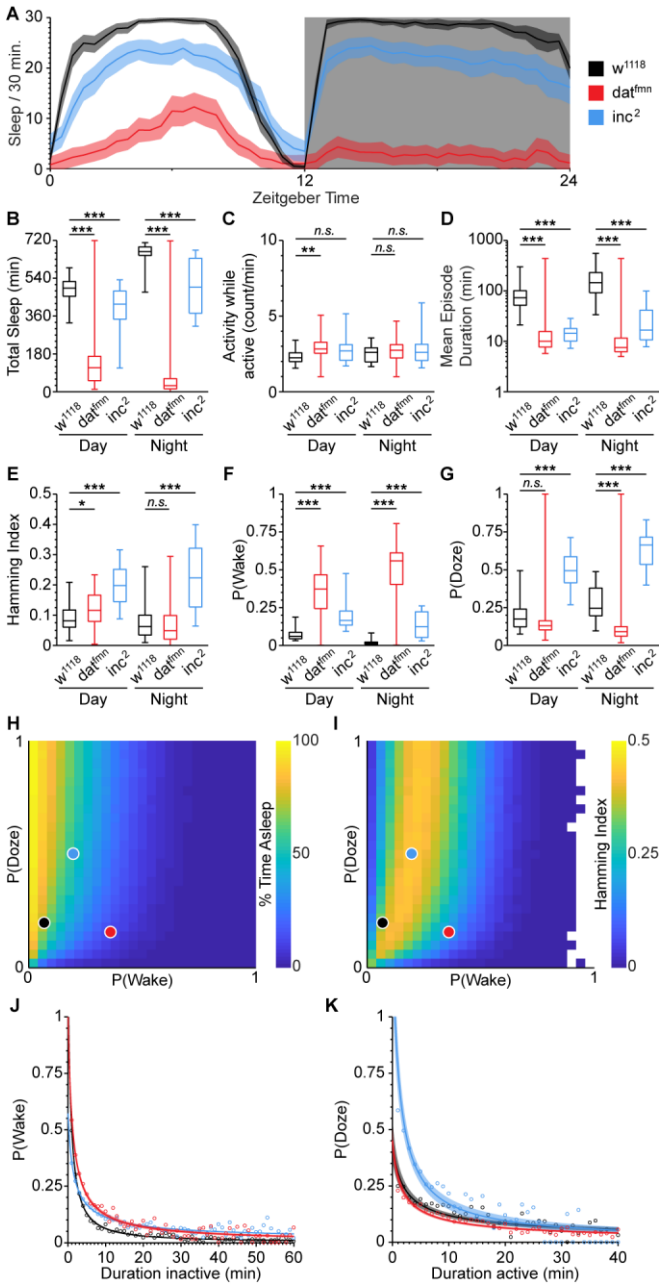

818

819 **Figure 7 - Mutations Affecting Sleep Act Through Both Wake and Doze**

820 **Probability.** (A) Circadian profile of sleep in a 12:12 Light:Dark cycle. Shaded regions

821 indicate lights on and lights off times. Lines are the population average, shaded area is

822 the 95% confidence interval of the mean. Individual profiles are the average of 3 days of

823 behavior. (B-G) Box and whisker plots of total sleep (B), activity while awake (C), mean

824 sleep episode duration (D), Hamming index (E), P(Wake) (F), and P(Doze) (G). Boxes

indicate the 25/50/75th percentiles for each group, whiskers indicate the minimum and maximum. (H,I) Heatmaps of simulated sleep at each level of P(Wake) and P(Doze), reproduced from Fig. 2. Circles indicate the coordinates of the mean P(Wake) and P(Doze) of the control (w^{1118}; black), *fumin* (red), and *insomniac* (blue) flies during daytime. (J,K) Power law function fits of P(Wake) and P(Doze) of each genotype during daytime. w^{1118}: black, *fumin*: red, *insomniac*: blue. Open circles are the empirical data, lines are the best fit, and shaded regions are the 95% prediction bounds for the fit. *n.s.* indicates no significant difference, * $p < 0.05$, ** $p < 0.005$, *** $p < 0.0005$.

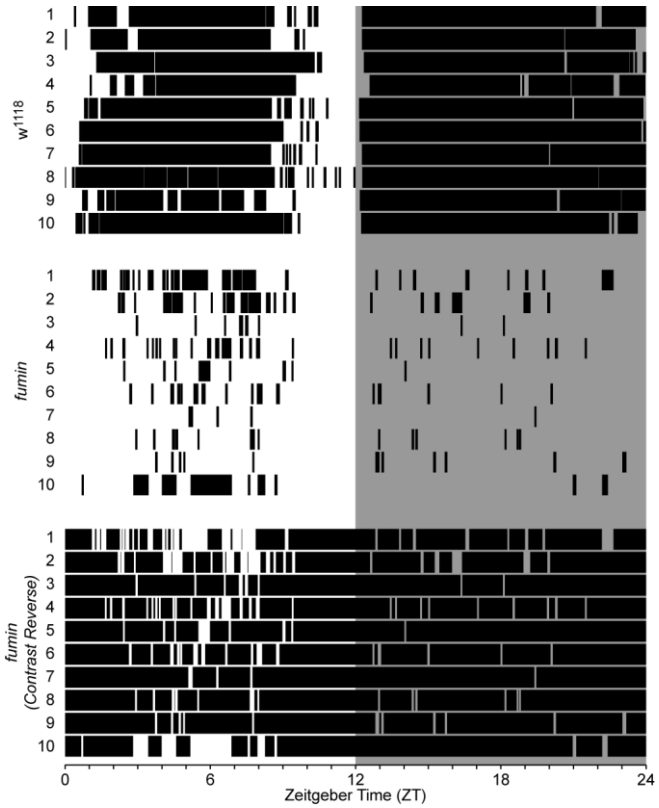

Figure S1 – Sleep Rasters of Control and *fumin* flies. 24 hours sleep rasters of ten w^{1118} flies (Top) and ten *fumin* flies (Middle and Bottom). In the top two sets of rasters, white is wake, black is sleep. In the bottom set of rasters, white is sleep and black is wake. The gray filled area is night.